Indian Journal of Pure & Applied Physics
Vol. 60, March 2022, pp. 268-273

The Hyades Kinematical Structure with Gaia Era

Amnah S. Al-Johani[a], W. H. Elsanhoury[b,c]*, Aneefah Al-Anzi[a], Bashayr Al-Jaber[a], Fatmah Al-Bishi[a], Nourah Kanaan[a], Ragwa Al-Atwi[a], Reem Al-Khubrani[a] & Sarah Al-Anzi[a]

[a]Mathematics Department, Faculty of Science, Tabuk University, Saudi Arabia

[b]Astronomy Department, National Research Institute of Astronomy and Geophysics (NRIAG) 11421, Helwan, Cairo, Egypt

[c]Physics Department, Faculty of Science and Arts, Northern Border University, Turaif Branch, Saudi Arabia

Received 31 December 2021; accepted 31 January 2022

In this work, we have improved the Hyades members with crossmatch between Hipparcos and the recent Gaia EDR3 source, the obtained members with highly probable are about 186 candidates. Considering the classical convergent point and depending on proper motions and radial velocities, we have computed the apex position $(A_{cp}, D_{cp}) = (93^o.36 \pm 0^o.046, 7^o.43 \pm 0^o.713)$ which is in line with others. The internal structural parameters of the Hyades open cluster are demonstrated here with space spatial velocities; i.e., $(\overline{V}_X, \overline{V}_Y, \overline{V}_Z;\ \mathrm{km\ s^{-1}})$ =(-5.97±0.41, 45.54±6.75, 5.52±0.43) and $(\overline{U}, \overline{V}, \overline{W};\ \mathrm{km\ s^{-1}})$ = (-42.11±6.50, -19.09±4.37, -1.32±0.44) and on basis of matrix elements (μ_{ij}), the Velocity Ellipsoid Parameters were achieved, *e.g.*, $(\lambda_1, \lambda_1, \lambda_1;\ \mathrm{km\ s^{-1}}) = (2137.36 \pm 23.12, 6.06 \pm 0.41, 2.53 \pm 0.63)$ and $(\sigma_1, \sigma_1, \sigma_1;\ \mathrm{km\ s^{-1}}) = (46.23 \pm 6.80, 2.47 \pm 0.64, 1.59 \pm 0.80)$.

For the observational quantities, we have deduced a correlation coefficient of about ≈ 0.83 for the kinematical property of proper motions on both sides $(\mu_\alpha \cos\delta, \mu_\delta;\ \mathrm{mas\ yr^{-1}})$ and the physical property with the angular distances (λ) from the vertex, and those prove that the attributes are completely related linearly.

Keywords: Stars kinematics and dynamics, Stars distances, Galaxy structure

1 Introduction

The present work deals with studying the moving open stellar clusters (OCs), which are an assembly of stars in a limited volume of space within the Galactic system characterized by the parallelism equality of their motions, these physically related groups held together by mutual gravitational attraction. Therefore, they populate a limited region of space, typically much smaller than their distance from us, so that they are all roughly at the same distance. As is well known, determining distances is the most fundamental step to measuring cluster ages and other key properties[1].

OCs are important laboratories for testing stellar evolution models and for describing the star formation history of our Milky Way (MW) Galaxy since each cluster contains samples of stars of single age and (probably) composition.

The distance to the Hyades has for many years been based solely on the convergent point method until[2] suggested that the cluster was located some 20 % farther from the Sun than indicated by the proper motion.

Various methods used for determining the Hyades distance modulus were reviewed[3], *e.g.*, proper motions, trigonometric parallaxes of Hyades members, dynamical parallaxes, the Ca II K-line absolute magnitudes, photometric parallaxes, and stellar-interior calculations. He concluded that all "secondary" distance indicators yield distance moduli greater than those determined from proper motions. A weighted value of (m – M) = 3.21±0.03 is adopted as the best distance modulus for the Hyades.

The present work aims to estimate the Hyades vertex with the classical convergent point method and based on the astrometric parameters in line with the Gaia EDR3 (hereafter EDR3).

An intrinsic relation was developed[4] for Hyades member stars between a function of the right ascensions (α) and declination (δ) with the angular distance (λ) from the vertex with a correlation coefficient of value ≈ 1. Recently[5], deduced an intrinsic relation for Hyades with Gaia between their luminosity function $\Phi(M_V)$ & $\Psi(M_V)$ and the absolute magnitudes (M_V) (*i.e.*, the linear correlation coefficient ≈ 0.995). On the other hand, the intrinsical relationship was developed here between the members' proper motions in both directions $(\mu_\alpha \cos\delta, \mu_\delta;\ \mathrm{mas\ yr^{-1}})$ and their angular distances (λ) from the vertex.

In the present paper, the data are achieved with Section 2. Section 3 deals with vertex determination

*Corresponding author:
(E-mail: welsanhoury@gmail.com)

and kinematical structure. The fourth Section presents the intrinsic relationship between proper motion and angular distance from the vertex. Finally, the conclusion attention with Section 5.

2 Data extraction

To perform the present analysis, we have extracted some of the astrometric data which serve our purpose of calculations with the third intermediate Gaia Data Release (Gaia EDR3).

EDR3[6] was planned for the first half of 2022 and was made public on 2020 December 3rd. for row data that was collected by the European Space Agency's Gaia mission during its first 34 months of continuous scanning over the sky by the Gaia Data Processing and Analysis Consortium (DPAC). EDR3 is setting a recent major achievement for Gaia's mission in stellar, Galactic, and extra Galactic analysis. In this release, the source evolution is stabilized with far fewer changes in the source list between Gaia DR2 and EDR3 than between Gaia DR1 and Gaia DR2; 97.5% of the sources persist.

Although the number of sources in the EDR3 catalog is only slightly larger than that of Gaia DR2, the cyclic nature of the Gaia DPAC processing means that the new release is based on a complete reprocessing of the mission data, allowing it to benefit from substantial improvements in the various Charge-Coupled Device (CCD) calibrations, instrument models, and photometric and astrometric calibrations. EDR3 will provide much more comprehensive information, like; radial (line of sight) velocities, many sets of data with different classes of variable sources, complementary astrometric data on extended and non-single objects, and classification and astrophysical parameters for different subsets of sources.

EDR3 consists of five quantities, which are central coordinates (α, δ), the proper motions in the two directions $(\mu_\alpha \cos\delta, \mu_\delta;\ \mathrm{mas\,yr^{-1}})$, and the trigonometric parallaxes $(\pi;\ \mathrm{mas})$ for almost 2.5 billion[7] of stars and non-stellar sources with a limiting magnitude of 3 – 21 mag in G band as well as the line of sight velocity (V_r). The quality of the Gaia astrometry is unprecedented: errors on the EDR3 measurements are of the order of 10 – 100 μas and 20 – 140 μas yr^{-1} on proper motions[8]. The data are complemented by three bands (G, G_{BP}, and G_{RP}) photometry[9] covering the optical range from 330 – 1050, 330 – 680, and 630 – 1050 nm, respectively [10], better background estimation has been carried out in all these three passbands.

The number of observations available for a given source is, on average, larger than in Gaia DR2. The uncertainties in parallaxes are up to 0.02 – 0.03 mas for sources at G ≤ 15 mag and ~ 0.07 mas for sources with G ~ 17 mag. The uncertainties in EDR3 proper motion components are up to 0.01 – 0.02 mas yr^{-1} for G < 15 mag, and 0.4 mas yr^{-1} for G ~ 20 mag. The photometric errors in EDR3 passbands versus G magnitudes are plotted in the lower panel of Fig. 1 While the upper panel of the same plot gives the proper motion and their corresponding errors as a function of G magnitudes, showing that the maximum error in proper motion components is 1.6 mas yr^{-1} for G ≤ 20 mag and 0.71 mas yr^{-1} for G ≤ 17.

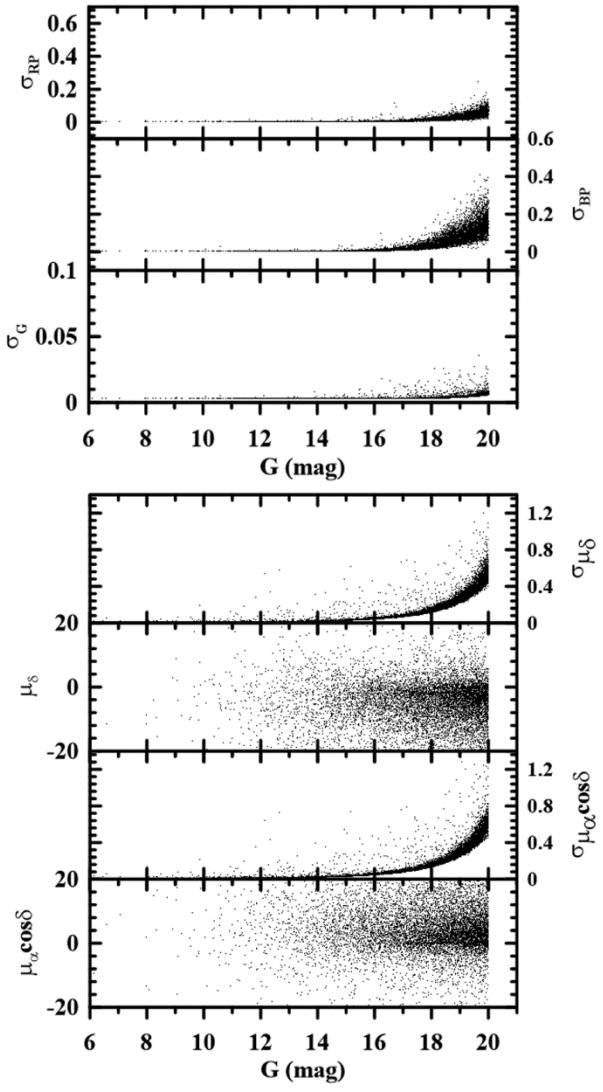

Fig. 1— The photometric errors (σ_G, σ_{BP}, and σ_{RP}) *vs.* G mag *(upper panel)* and the plot of the proper motions in the two directions with their errors $\left(\sigma_{\mu_\alpha \cos\delta}, \sigma_{\mu_\delta}\right)$ *vs.* G mag *(lower panel)*.

Crossmatch (XM) solution implemented for the EDR3 with 78 billion processed transits[7], this updated merging XM is crucial for the performance of both astrometric and photometric parameters because it provides the matched observations that are to be used in the subsequent pipelines within the Gaia DPAC. As compared with the Gaia DR2; the detection classification was more improved significantly around bright sources with the revision of the transit classification model parameters. Moreover, an additional module has been included that provides a cluster classification based on the quality of the transit windows. It prevents the creation of new sources when most of the cluster transits are dubious.

The Hyades OC Gaia's members (N=186) were gotten through[11] whose linkage between Hyades Hipparcos identification (HIP) was devoted with [12] and the EDR3 source.

3 Hyades apex (A_{cp}, D_{cp}) and its kinematical structure

3.1 The classical convergent point (A_{cp}, D_{cp})

For a group of 186 Hyades member stars located with equatorial coordinates (α, δ), at a distance r_i (pc), proper motions in RA and DEC as $(\mu_\alpha \cos\delta, \mu_\delta;\ \text{mas yr}^{-1})$, and the radial velocity $(V_r;\ \text{km s}^{-1})$ are used in this analysis. Considering the above parameters, we can estimate the velocity components $(V_x, V_y, V_z;\ \text{km s}^{-1})$ along x, y, and z axes in the coordinate system centered at the Sun and according to the well-known formulae given by[13].

$$V_x = -4.74 r_i \mu_\alpha \cos\delta \sin\alpha - 4.74 r_i \mu_\delta \sin\delta \cos\alpha + V r \cos\delta \cos\alpha, \quad \ldots (1)$$

$$V_y = +4.74 r_i \mu_\alpha \cos\delta \cos\alpha - 4.74 r_i \mu_\delta \sin\delta \sin\alpha + V r \cos\delta \sin\alpha, \quad \ldots (2)$$

$$V_z = +4.74 r_i \mu_\delta \cos\delta + V_r \sin\delta. \quad \ldots (3)$$

From the above equations and letting

$$\xi = \frac{V_X}{V_Y}, \quad \ldots (4)$$

$$\eta = \frac{V_Y}{V_Z}, \quad \ldots (5)$$

we get

$$a_i \xi + b_i \eta = c_i, \quad \ldots (6)$$

where the coefficients

$$a_i = \mu_\alpha^{(i)} \sin\delta_i \cos\alpha_i \cos\delta_i - \mu_\delta^{(i)} \sin\alpha_i,$$
$$b_i = \mu_\alpha^{(i)} \sin\delta_i \sin\alpha_i \cos\delta_i + \mu_\delta^{(i)} \cos\alpha_i, \quad \ldots (7)$$
$$c_i = \mu_\alpha^{(i)} \cos^2_{\delta_i}.$$

and the index (i) varies from 1 to (N) which is the number of cluster members. So

$$\tan A_{cp} = \frac{\eta}{\xi}, \quad \ldots (8)$$

$$\tan D_{cp} = (\xi^2 + \eta^2)^{-1/2}, \quad \ldots (9)$$

The required vertex coordinates (A_{cp}, D_{cp}) of the cluster, follows directly from Eq.s (8 and 9).

3.2 The Hyades kinematical structure

It's known that the importance of the OCs is the first step for studying and investigating the stellar and Galactic structures. Inside the contour of the OCs; since we have a distribution of residual velocities of stars, and to compute those velocity ellipsoids and their corresponding parameters based on the matrix elements (μ_{ij}), *e.g.*, space internal motions or called the dispersion velocities $(\sigma_j;\ \forall_j = 1,2,3)$, direction cosines $(l_j, m_j, n_j;\ \forall_j = 1,2,3)$, and the Galactic longitude and Galactic latitude parameters $(L_j, B_j;\ \forall_j = 1,2,3)$. The obtained results are given herewith in Table 1. A Mathematica routine has been developed to compute these kinematics and velocity ellipsoid parameters (VEPs) following the computational algorithm mentioned with [14, 15, 16], this mentioned algorithm depends on.

i) The space velocity components (U, V, W) along with Galactic coordinates as a function of space stellar velocities (V_x, V_y, V_z) whose definite to the Sun, a mathematical corresponding correlation between all of these former quantities; were derived by [17] based on Near Infra-Red (NIR) by 2 μm all-sky survey catalog (2MASS) [18] and the radio observation data; i.e.

$$U = -0.0518807421\, V_x - 0.872222642\, V_y - 0.4863497200\, V_z, \quad \ldots (10)$$

$$V = +0.4846922369\, V_x - 0.4477920852\, V_y + 0.5713692061 V_z, \quad \ldots (11)$$

$$W = -0.8731447899\, V_x - 0.1967483417\, V_y + 0.4459913295\, V_z. \quad \ldots (12)$$

while the mean velocities are defined as.

$$\overline{U} = \frac{1}{N}\sum_{i=1}^{N} U_i, \overline{V} = \frac{1}{N}\sum_{i=1}^{N} V_i, \overline{W} = \frac{1}{N}\sum_{i=1}^{N} W_i.$$

Table 1 — The Hyades kinematical structure parameters with Gaia EDR3.

(A_{cp}, D_{cp})	$93^o.36 \pm 0^0.046, 7^o.43 \pm 0^o.71$	Present study
	$96^o.00 \pm 1^o.00, 5^o.66 \pm 0^o.12$	[20]
	$97^o.00 \pm 1^o.00, 7^o.00 \pm 0^o.70$	[21]
	$97^o.91, 6^o.66$	[12]
V (km/s)	42.23 ± 6.50	Present study
	46.97	[12]
d (pc)	48.43 ± 6.96	Present study
	46.34	[12]
$(\bar{V}_X, \bar{V}_Y, \bar{V}_Z)$ (km/s)	$-5.97 \pm 0.41, 45.54 \pm 6.75, 5.52 \pm 0.43$	Present study
	-5.43, 46.08, 4.52	[20]
$(\bar{U}, \bar{V}, \bar{W};\ \mathrm{km\ s^{-1}})$	$-42.11 \pm 6.50, -19.09 \pm 4.37, -1.32 \pm 0.44$	Present study
	-42.14, -19.80, -2.35	[20]
$(\lambda_1, \lambda_2, \lambda_3)$ (km/s)	$2137.36 \pm 23.12, 6.06 \pm 0.41, 2.53 \pm 0.63$	Present study
$(\sigma_1, \sigma_2, \sigma_3)$ (km/s)	$46.23 \pm 6.80, 2.47 \pm 0.64, 1.59 \pm 0.80$	Present study
$(l_1, m_1, n_1)^o$	0.9109, 0.4117, 0.0290	Present study
$(l_2, m_2, n_2)^o$	-0.2674, 0.6423, -0.7183	Present study
$(l_3, m_3, n_3)^o$	0.3143, -0.6466, -0.6952	Present study
(x_c, y_c, z_c) (pc)	$18.17 \pm 4.26, 41.93 \pm 6.48, 13.98 \pm 3.74$	Present study
	18.00, 42.00, 14.00	[20]
B_1	1.66 ± 0.30	Present study
B_2	-45.92 ± 6.78	Present study
B_3	-44.04 ± 6.64	Present study
L_1	-24.32 ± 4.93	Present study
L_2	-112.61 ± 10.61	Present study
L_3	-115.93 ± 10.77	Present study
$X_\odot$ (kpc)	-0.045 ± 0.002	Present study
	-0.044 ± 0.002	[20]
	-0.046	[22]
$Y_\odot$ (kpc)	-0.00005 ± 0.0001	Present study
	-0.004 ± 0.0001	[20]
	-0.00005	[22]
$Z_\odot$ (kpc)	-0.019 ± 0.001	Present study
	-0.018 ± 0.001	[20]
	-0.0014	[22]
R_{gc} (kpc)	8.245 ± 0.60	Present study
	7.50 ± 0.60	[20]
	8.50	[23]

Terms of the (3×3) matrix elements (μ_{ij}) that controls the eigenvalue problem $[D(\lambda) = |B - \lambda I| = 0]$ for the velocity ellipsoid, i.e.

$$\boldsymbol{\mu_{11}} = \frac{1}{N}\sum_{i=1}^{N} U_i^2 - (\bar{U})^2\,; \quad \boldsymbol{\mu_{12}} = \frac{1}{N}\sum_{i=1}^{N} U_i V_i - \bar{U}\bar{V};$$

$$\mu_{13} = \frac{1}{N}\sum_{i=1}^{N} U_i W_i - \bar{U}\bar{W}\,; \quad \mu_{22} = \frac{1}{N}\sum_{i=1}^{N} V_i^2 - (\bar{V})^2;$$

$$\mu_{31} = \frac{1}{N}\sum_{i=1}^{N} V_i W_i - \bar{V}\bar{W}\,; \quad \mu_{33} = \frac{1}{N}\sum_{i=1}^{N} W_i^2 - (\bar{W})^2;$$

where, (N) is the number of member stars, (λ) is the eigenvalue and (B) could be written as.

$$B = \begin{vmatrix} \mu_{11} & \mu_{12} & \mu_{13} \\ \mu_{12} & \mu_{22} & \mu_{23} \\ \mu_{13} & \mu_{23} & \mu_{33} \end{vmatrix}.$$

a) The direction cosines parameters

The direction cosines $(l_j, m_j, n_j, \forall j = 1,2,3)$ for the eigenvalue problem (λ_j), matrix elements (μ_{ij}), and dispersion velocities (σ_j) $[\text{i.e. } \sigma_j = \sqrt{\lambda_j}, \forall j = 1,2,3]$ along three axes [19] is mathematically given by the following:

$$l_j = \left[\mu_{22}\mu_{33} - \sigma_j^2(\mu_{22} + \mu_{33} - \sigma_j^2) - \mu_{23}^2\right]/D_j, \ldots (13)$$

$$m_j = \left[\mu_{23}\mu_{13} - \mu_{12}\mu_{33} + \sigma_j^2\mu_{12}\right]/D_j, \quad \ldots (14)$$

$$n_j = \left[\mu_{12}\mu_{23} - \mu_{13}\mu_{22} + \sigma_j^2\mu_{13}\right]/D_j, \quad \ldots (15)$$

where $(l_j^2 + m_j^2 + n_j^2 = 1)$ as an initial test for our code for our sample and,

$$D_j^2 = (\mu_{22}\mu_{33} - \mu_{23}^2)^2 + (\mu_{23}\mu_{13} - \mu_{12}\mu_{33})^2 + (\mu_{12}\mu_{23} - \mu_{13}\mu_{22})^2 + 2[(\mu_{22} + \mu_{33})(\mu_{23}^2 + \mu_{22}\mu_{33}) + \mu_{12}(\mu_{23}\mu_{13} - \mu_{12}\mu_{33}) + \mu_{13}(\mu_{12}\mu_{23} - \mu_{13}\mu_{22})]\sigma_j^2 + (\mu_{33}^2 + 4\mu_{22}\mu_{33} + \mu_{22}^2 - 2\mu_{23}^2 + \mu_{12}^2 + \mu_{13}^2)\sigma_j^4 - 2(\mu_{22} + \mu_{33})\sigma_j^6 + \sigma_j^8.$$

b) The velocity of the cluster

The velocity (V) of the cluster may be presented as a function of the line-of-sight velocity (V_r) and the angular distance of the star from the vertex (λ_i) like,

$$V = \left[\frac{\sum_{i=1}^{N} V_r^{(i)} \cos\lambda_i}{\sum_{i=1}^{N} \cos^2\lambda_i}\right], \quad \ldots (16)$$

into which

$$\lambda_i = \cos^{-1}\left[\sin\delta_i \sin D_{cp} + \cos\delta_i \cos D_{cp} \cos(A_{cp} - \alpha_i)\right]. \quad \ldots (17)$$

c) The Galactic longitude and Galactic latitude parameters

Let (L_j) and (B_j), $(\forall j = 1,2,3)$ be the Galactic longitude and the Galactic latitude of the directions, respectively which correspond to the extreme values of the dispersion, then

$$L_j = \tan^{-1}\left(\frac{-m_j}{l_j}\right), \quad \ldots (18)$$

$$B_j = \sin^{-1}(n_j). \quad \ldots (19)$$

d) The center of the cluster

The center of the cluster (x_c, y_c, z_c) can be derived by the simple method of finding the equatorial coordinates of the center of mass for the number (N_i) of discrete objects, *i.e.*

$$x_c = \frac{\sum_{i=1}^{N} r_i \cos\alpha_i \cos\delta_i}{N}, \quad \ldots (20)$$

$$y_c = \frac{\sum_{i=1}^{N} r_i \sin\alpha_i \cos\delta_i}{N}, \quad \ldots (21)$$

$$z_c = \frac{\sum_{i=1}^{N} r_i \sin\delta_i}{N} \quad \ldots (22)$$

e) The distance of the cluster

Since the distance $d(pc)$ is the reciprocal of the parallax (p), then the distance of the cluster has the following form

$$d = N/\sum_{i=1}^{N} p_i. \quad \ldots (23)$$

f) The projected distances

Considering our estimated distances $d(pc)$ we infer to include those distances to the Galactic center (R_{gc}) using $R_{gc} = \sqrt{R_o^2 + (d\cos b)^2 - 2R_o d\cos b\cos l}$, where $R_o = 8.20 \pm 0.10$ kpc[24]. After that, the anticipated (projected) distances towards the Galactic plane $(X_\odot, Y_\odot)$ and the distance from the Galactic plane $(Z_\odot)$ maybe computed as:

$$X_\odot = d\cos b\cos l,$$

$$Y_\odot = d\cos b\sin l, \quad \ldots (24)$$

$$Z_\odot = d\sin b.$$

4 The intrinsic relationship between $q(\mu_\alpha\cos\alpha, \mu_\delta)$ and (λ)

In what follows, we may retrieve a very significant relationship between Hyades proper motion in both directions, *i.e.*, $q(\mu_\alpha\cos\alpha, \mu_\delta)$ and the angular distance $(\lambda_{cal.})$ of the star from the vertex, is relation is given as.

$$\lambda_{cal.} = C_1 + C_1 q. \quad \ldots (25)$$

where

$$q = \frac{\mu_\delta\sin\delta - \mu_\alpha\cos\alpha}{\mu_\delta\cos\delta - \mu_\alpha\sin\alpha} \quad \ldots (26)$$

Graphically we may get the correlation between angular distance (λ) versus $q(\mu_\alpha\cos\alpha, \mu_\delta)$ as shown in Fig. 2, where the coefficients and their probable errors are:

- $C_1 = 0.247305 \pm 0.005751$
- $C_2 = 0.35323 \pm 0.0119044$
- The probable error of the fit is $e = 0.030$
- The average squared distance between the exact solution and the least-squares solution Q [25] $= 0.000384179$
- The linear correlation coefficient between $(q, \lambda_{cal.})$ is $r = 0.828$
- The graphical representation between the raw data and the fitted data with its relative
- errors $\left(\text{i.e.}, \Delta = \frac{\lambda_{obs.} - \lambda_{cal.}}{\lambda_{cal.}}\right)$ was ranged between -0.435 and 0.456.

Some statistical analyses of the relationship are given as follows:

- Mean (average value) = -0.002269
- Median (central value) = 0.0131132
- Variance $= \frac{1}{N}\sum_{i=1}^{N}(\Delta_i - \bar{\Delta})^2$ = 0.0113084
- Median absolute deviation = median of $|\Delta_i - median|$ = 0.0395812
- Root mean square $= \sqrt{\frac{1}{N}\sum_{i=1}^{N}\Delta_i^2}$ = 0.106079
- Mean absolute deviation $= \frac{1}{N}\sum_{i=1}^{N}|\Delta_i - \bar{\Delta}|$ = 0.0700062

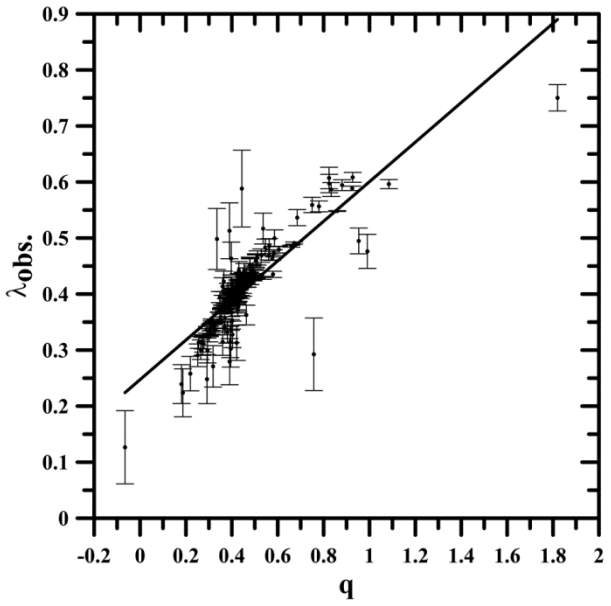

Fig. 2— The graphical representation between the angular distance from the vertex $(\lambda_{obs.})$ and the proper motion in both directions $q(\mu_\alpha\cos\alpha, \mu_\delta)$ with its error bars

5 Conclusion

This work may be summarized as follows.

- By cross-correlation, we improved the Hyades's open cluster Hipparcos members with the more recent data source (i.e., Gaia EDR3) to get 186 candidates.
- Computations of spatial velocities along x, y, and z; $(\overline{V}_X, \overline{V}_Y, \overline{V}_Z;\ \mathrm{km\ s^{-1}})$ =(-5.97±0.41, 45.54±6.75, 5.52±0.43) and those along with Galactic coordinates; $(\overline{U}, \overline{V}, \overline{W};\ \mathrm{km\ s^{-1}}) =$ (-42.11±6.50, -19.09±4.37, -1.32±0.44) are in line with those previously obtained in the literature.
- To compute the coordinates of the gathered coherent point (vertex) with the classical convergent point method, we developed our routine and deduced the results, $(A_{cp},\ D_{cp}) = (93^{\circ}.36 \pm 0^{\circ}.046, 7^{\circ}.43 \pm 0°.713$, which is in line with published ones.
- For Hyades OC and depending on the matrix elements (μ_{ij}), we have computed the Velocity Ellipsoid Parameters (VEPs) such as dispersion velocities $(\sigma_j;\ \forall_j = 1,2,3)$, direction cosines $(l_j, m_j, n_j;\ \forall_j = 1,2,3)$, the Galactic longitude of the vertex (l_2), and the Solar elements. The obtained results are listed in Table 1.
- Finally, we have deduced a correlation between the members' Galactic coordinates $q(\mu_\alpha \cos\delta, \mu_\delta)$ and the angular distances (λ) from the vertex. A correlation coefficient of value ≈ 0.83 was found, which proves that the attributes are completely related linearly.

Acknowledgments

The authors are deeply thankful to the referees of this paper for their valuable and many useful constructive comments that improved the original manuscript.

This work presents results from the European Space Agency (ESA) space mission Gaia. Gaia data are being processed by the Gaia Data Processing and Analysis Consortium (DPAC). Funding for the DPAC is provided by national institutions, in particular the institutions participating in the Gaia Multi-Lateral Agreement (MLA). The Gaia mission website is https://www.cosmos.esa.int/gaia. The Gaia archive website is https://archives.esac.esa.int/gaia.

References

1 Pinsonneault M H, Terndrup D M, Hanson R & Stauffer J R, *Astrophys J*, 600 (2004) 946.
2 Hodge P W & Wallerstein G A, *Astron Soc Pacific*, 78 (1966) 411.
3 van Altena W F, *Astron Soc Pacific*, 86 (1974) 217.
4 Sharaf M A & Selim H H, *Int J Astron Astrophys*, 1 (2011) 104.
5 Elsanhoury W H, Al-Johani A S, El Fewaty N H, et al., *Contributions of the Astronomical Observatory Skalnaté Pleso*, 52 (2022) 32.
6 Brown A G A, Vallenari A, Prusti T, de Bruijne J H J, Babusiaux C, Biermann M, et al., *Astron Astrophys*, 649 (2020) A1.
7 Torra F, Castañede J, Fabricius C, Lindegren L, Clotet M, González-Vidal J J, et al., *Astron Astrophys*, 649 (2021) A10.
8 Lindegren L, Kiloner S A, Hernández J, et al., *Astron Astrophys*, 649 (2021) A2.
9 Riello M, De Angeli F, Evans D E, et al., *Astron Astrophys*, 649 (2021) A3.
10 Evans D W, Riello M, De Angeli F, et al., *Astron Astrophys*, 616 (2018) A4.
11 Brandt T D, *Astrophys J Suppl*, 254 (2021) 42.
12 Perryman M A C, Brown A G A, Lebreton Y, Gomez A, Turon C & Cayrel de Strobel G, *Astron Astrophys*, 331 (1998) 81.
13 Smart W M, *Stellar Dynamics. London: Longmans* (1968).
14 Elsanhoury W H, *J Astrophys Astron*, 42 (2021) 90.
15 Elsanhoury W H, Nouh M I & Abdel-Rahman H I, *Revista Mexicana de Astronomía y Astrofísica*, 51 (2015) 199.
16 Bisht D, Elsanhoury W H, Qingfeng Z, et al., *Astron J*, 160 (2020) 119.
17 Liu J C, Zhu Z & Hu B, *Astron Astrophys*, 536 (2011) A102.
18 Skrutskie M F, Cutri R M, Stiening R, at al., *Astron J*, 131 (2006) 1163.
19 Elsanhoury W H, Postnikova E S, Chupina N V, Vereshchagin S V, Sariya D P, Yadav R K S, et al., *Astrophys Space Sci*, 363 (2018) 58.
20 Elsanhoury W H & Nouh M I, *New Astron*, 72 (2019) 19.
21 Vereshchagin S V, Reva V G & Chupina N V, *Astron Rep*, 52 (2008) 94.
22 Kharchenko N V, Piskunov A E, Schilbach E, Röeser S & Scholz R-D, *Astron Astrophys*, 585 (2016) A101.
23 Röser S, Schilbach E, Piskunov A E, Kharchenko N V & Scholz R-D, *Astron Astrophys*, 531 (2011) A92.
24 Bland-Hawthorn J, Sharma S, Tepper-Garcia T, Binney J, Freeman K C, Hayden M R, et al., *Monthly Notes Royal Astron Soc,* 486 (2019) 1167.
25 Kopal Z & Sharaf M A, *Astrophys Space Sci*, 70 (1980) 77.